# OPTIMISATION OF THE BEAM LINE FOR COMET PHASE-I

A. Kurup, I. Puri, Y. Uchida, Y. Yap, Imperial College London, UK
R. B. Appleby, S. Tygier, The University of Manchester and the Cockcroft Institute, UK
R. D'Arcy, A. Edmonds, M. Lancaster, M. Wing, UCL, UK

*Abstract*

The COMET experiment will search for very rare muon processes that will give us an insight into particle physics beyond the Standard Model. COMET requires an intense beam of muons with a momentum less than 70 MeV/c. This is achieved using an 8 GeV proton beam; a heavy metal target to primarily produce pions; a solenoid capture system; and a curved solenoid to perform charge and momentum selection.

It was recently proposed to build COMET in two phases with physics measurements being made in both phases. This requires re-optimising the beam line for a shorter curved solenoid. This will affect the pion and muon yield; the momentum distributions at the detector; and the collimator scheme required. This paper will present the beam line design for COMET Phase-I, which aims to maximise the yield for low momentum muons suppressing sources of backgrounds in the beam.

## INTRODUCTION

The COherent Muon to Electron Transition (COMET) experiment [1] aims to measure the conversion of muons to electrons in the presence of a nucleus. This process is forbidden by the Standard Model (SM) of particle physics. However, models that go beyond the SM such as supersymmetric theories predict this process to exist with a branching ratio that may be in the range $10^{-13}$–$10^{-15}$ [2]. COMET aims to achieve a sensitivity of $< 10^{-16}$ and thus will be able to observe conversions at this level. It was recently decided to construct the COMET experiment in two stages, with the ability to search for muon to electron conversion in both stages.

COMET Phase-I will allow performance measurements of the beam line, which will be very important to understand sources of backgrounds for COMET Phase-II. Searching for muon to electron conversion in COMET Phase-I, however, requires re-optimising the beam line. Figure 1 shows the layout of COMET Phase-I. The beam line up to the end of the muon torus will be the same as COMET Phase-II.

The muon torus in Phase-I only bends through 90° whereas in Phase-II there are two 90° sections. This means the separation of particles caused by the vertical dispersion of the bent solenoid will be less in Phase-I. Thus, the beam will contain more background particles that could fake the signal of muon to electron conversion. The number of background particles could be reduced by re-optimising the dipole field applied over the length of the muon torus and re-optimising the beam collimator.

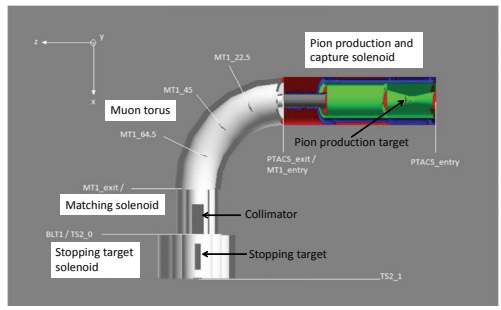


Figure 1: Schematic layout of COMET Phase-I.

## MAGNETIC FIELD

The beam line of Phase-I consists of a continuous solenoid channel with a peak field of 5T centered on the pion production target and tapers down to 3T at the entrance of the muon torus. The muon torus has a curved solenoid field that causes particles to drift vertically depending on their charge and momentum and this is used to elliminate high momentum particles and positively charged particles. The matching solenoid then tapers the field from 3T to match the 1T field of the muon stopping target solenoid. Figure 2 shows the field on-axis for COMET Phase-I.

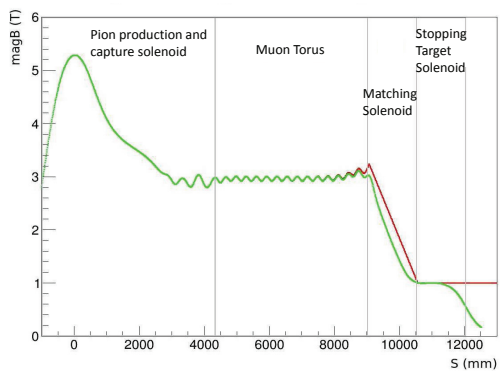


Figure 2: On-axis solenoid field for COMET Phase-I (green line). The red line shows a simplified, hard-edged, version of the matching and stopping target solenoid fields.

In addition to the solenoid field a dipole field is applied to prevent particles with the required central momentum from drifting vertically. Figure 3 shows the dipole field used in COMET Phase-II simulations. This is a hard-edged, uniform field. The dipole field can be produced using saddle-shaped coils in addition to the solenoid coils. This type of construction has been tested by the MuSIC project [3]. The magnitude of the dipole field (0.018 T)




ISBN 978-3-95450-122-9

was optimised for Phase-II to give the best muon yield but since the beam line in Phase-I is shorter this needs to be re-optimised.

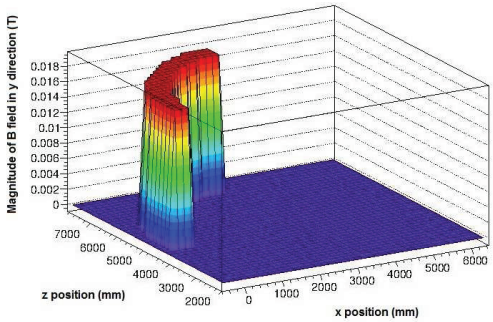


Figure 3: Dipole field applied to muon torus section.

The effect of varying the magnitude of the dipole field on the composition of the beam at the end of the muon torus was studied. Figure 4 shows the momentum distribution of negatively charged pions and muons and positvely charged muons for different multiples of the Phase-II dipole field. The number of primary protons used to produce these plots is $1 \times 10^6$. Varying the dipole field affects the ratio of useful muons and the potential background sources. High-momentum particles are more likely to produce high-momentum electrons that can fake the signal of muon to electron conversion and thus should be minimised. High-momentum is defined as: pions with a momentum greater than 80 MeV/c; muons with a momentum greater than 75 MeV/c; and electrons/positrons with a momentum greater than 100 MeV/c. Figure 5 shows the numbers of high-momentum particles for different dipole fields.

## COLLIMATOR

The aim of the collimator is to eliminate high-momentum particles from the beam that may produce high-momentum electrons that can fake the signal of muon to electron conversion. The collimator makes use of the vertical dispersion introduced by the muon torus, see Fig. 6.

The simulations performed here use the default value for the dipole field, which is 0.018 T. Figure 7 shows the momentum distributions of muons, pions and electrons just before the collimator (i.e. at the end of the muon torus).

The default schematic design for the beam collimator is shown in Fig. 8 and the placement of the collimator is shown in Fig. 1. For these simulations the parameter $R_{max}$ was set to 350 mm (the inner bore of the matching solenoid); $R_{min}$ was set to 200 mm (the inner bore of the muon torus); and the length was set to 1 m.

Figure 9 shows the effect of varying the $Y_{min}$ of a tungsten collimator on the momentum distribution of muons. The goal for the collimator is to have more of an effect on high-momentum particles. In these simulations, high-momentum particles are defined as: pions with momentum greater than 60 MeV/c; muons with momentum greater than 75 MeV/c; and electrons with momentum greater than 90 MeV/c. Figure 10 shows the percentage of high-momentum and low-momentum particles that are stopped by the tungsten collimator for different values of $Y_{min}$ and Fig. 11 shows this for an aluminium collimator. These plots also include the production of secondary electrons.

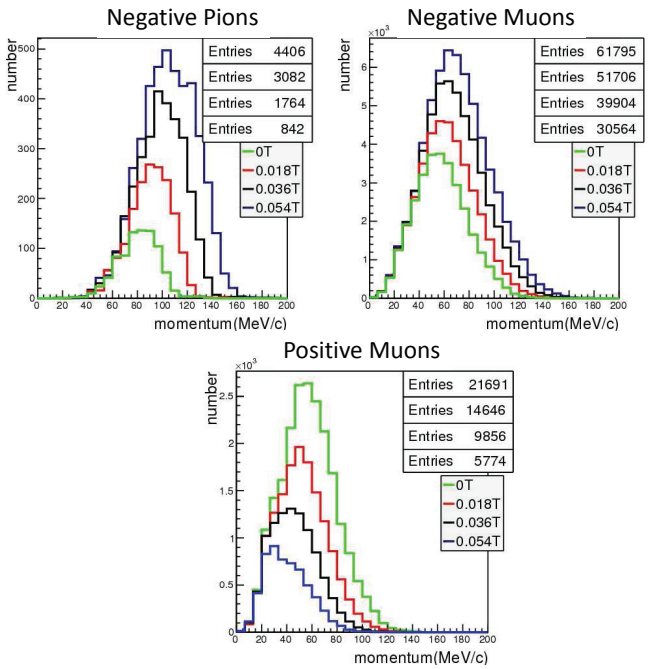


Figure 4: Momentum distribution of negative pions and muons and positively charged muons at the end of the muon torus for different dipole fields.

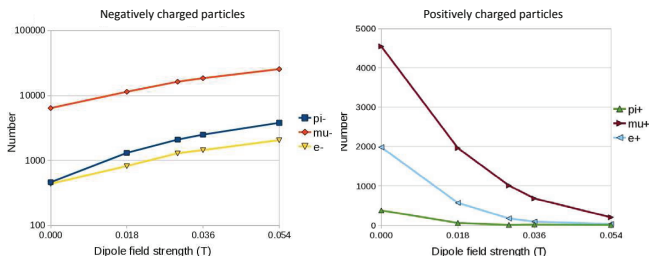


Figure 5: Numbers of high-momentum negatively charged (left) and positively charged (right) particles at the end of the muon torus as a function of dipole field.

## CONCLUSIONS

The effect of varying the dipole field over the muon torus and the effect of the beam collimator were studied independently. Studies of optimising the dipole field simultaneously with the collimator are on-going.

It was recently decided to change the material of the pion production target to graphite, as this would not need cooling and would therefore be cheaper. The target geometry will need to be re-optimised to maximise the pion yield

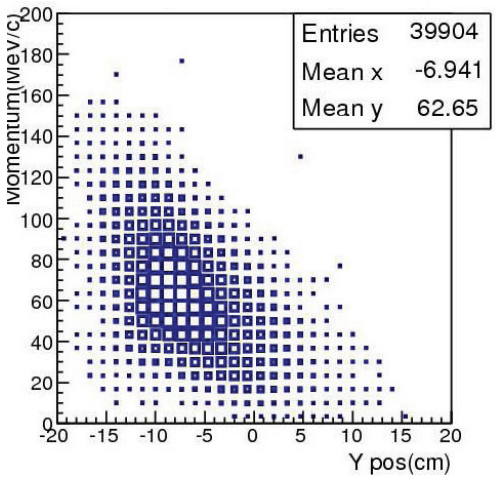


Figure 6: Dispersion of negatively charged muons after the muon torus with the default dipole field of 0.018 T.

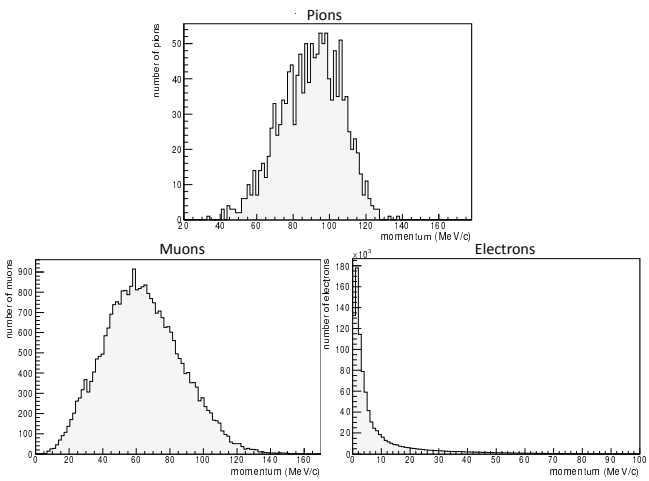


Figure 7: Momentum of muons, pions and electrons just before the collimator (i.e. after the muon torus).

and these beam line optimisations studies will need to be repeated.

## REFERENCES

[1] A. Kurup, "The COherent Muon to Electron Transition COMET Experiment.", In the Proceedings of the 1st International Particle Accelerator Conference: IPAC'10, Kyoto, Japan, 23-28 May 2010, p. 3470-3472.

[2] R. Kitano , M. Koike, S. Komine, Y. Okada, "Higgs-mediated muon electron conversion process in supersymmetric seesaw model", Phys. Lett. B **575**, 300 (2003).

[3] M. Yoshida, M. Fukuda, K. Hatanaka, Y. Kuno, T. Ogitsu, A. Sato, A. Yamamoto, "Superconducting Solenoid Magnets for the MuSIC Project", Applied Superconductivity, IEEE Transactions on , vol.21, no.3, pp.1752–1755, June 2011 doi: 10.1109/TASC.2010.2088360

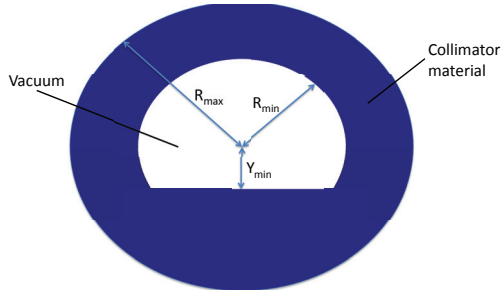


Figure 8: Schematic diagram of the COMET beam collimator.

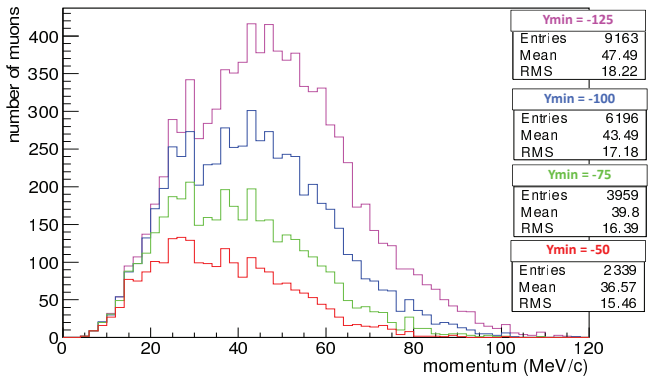


Figure 9: Momentum of muons after the tungsten collimator for different values of $Y_{min}$.

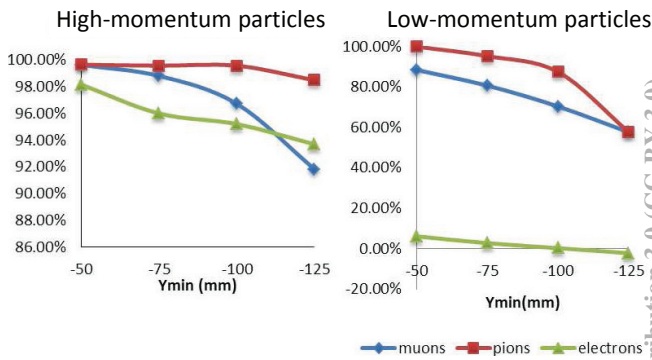


Figure 10: Percentage of high-momentum (left) and low-momentum (right) particles that are absorbed by the tungsten collimator for different values of $Y_{min}$.

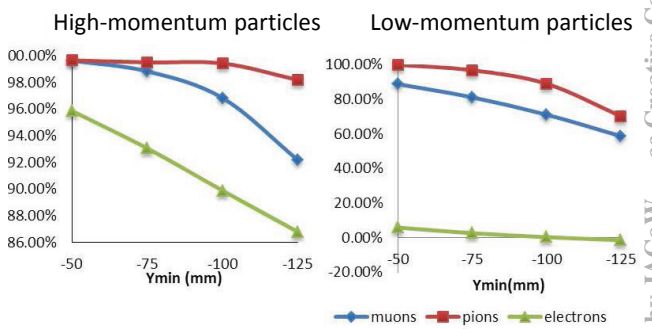


Figure 11: Percentage of high-momentum (left) and low-momentum (right) particles that are absorbed by the aluminium collimator for different values of $Y_{min}$.




ISBN 978-3-95450-122-9